Naval Research Laboratory

Stennis Space Center, MS 39529-5004

Validation Test Report for the Navy Standard Surf Model

Y. Larry Hsu

Ocean Dynamics and Prediction Branch
Oceanography Division

Theodore R. Mettlach
Marshall D. Earle

Neptune Sciences, Inc.
Slidell, Louisiana

June 21, 2002

Naval Research Laboratory

1. REPORT DATE (DD-MM-YYYY)	2. REPORT TYPE	3. DATES COVERED (From - To)
21-06-2002	Formal	

4. TITLE AND SUBTITLE

Validation Test Report for the Navy Standard Surf Model

5a. CONTRACT NUMBER

5b. GRANT NUMBER

5c. PROGRAM ELEMENT NUMBER
0603207N

6. AUTHOR(S)

Y. Larry Hsu, Theodore R. Mettlach,* and Marshall D. Earle*

5d. PROJECT NUMBER
X2343

5e. TASK NUMBER

5f. WORK UNIT NUMBER

7. PERFORMING ORGANIZATION NAME(S) AND ADDRESS(ES)

Naval Research Laboratory
Stennis Space Center, MS 39529-5004

8. PERFORMING ORGANIZATION REPORT NUMBER

NRL/FR/7322--02-10,008

9. SPONSORING / MONITORING AGENCY NAME(S) AND ADDRESS(ES)

Commander, Space and Naval Warfare Systems Command
PMW 185
4301 Pacific Highway OT-1
San Diego, CA 92110-3127

10. SPONSOR / MONITOR'S ACRONYM(S)

SPAWAR

11. SPONSOR / MONITOR'S REPORT NUMBER(S)

12. DISTRIBUTION / AVAILABILITY STATEMENT

Approved for public release; distribution is unlimited.

13. SUPPLEMENTARY NOTES

* Neptune Sciences, Inc., Slidell, LA 70461

14. ABSTRACT

This report documents the validation of wave height, longshore current, wave refraction, and shoaling computations for the Navy Standard Surf Model (NSSM). It also describes the improvements implemented in the latest version of NSSM, SURF 3.2. Previous comparisons with field data are summarized. Model wave height and longshore current estimates are also compared to two sets of laboratory measurements. Wave refraction and shoaling through transformation coefficients are evaluated by comparing mode results to corresponding results from a linear wave model. This report shows that SURF 3.2 is a robust and accurate model ready for delivery to the Oceanographic and Atmospheric Master Library (OAML).

15. SUBJECT TERMS

Wave refraction	OAML	NSSM	SURF 3.2
Surf	Military oceanography		

16. SECURITY CLASSIFICATION OF:			17. LIMITATION OF ABSTRACT	18. NUMBER OF PAGES	19a. NAME OF RESPONSIBLE PERSON
a. REPORT	**b. ABSTRACT**	**c. THIS PAGE**	SAR	31	Larry Hsu
Unclassified	Unclassified	Unclassified			**19b. TELEPHONE NUMBER** (include area code) 228-688-5260

CONTENTS

iii

VALIDATION TEST REPORT FOR THE NAVY STANDARD SURF MODEL

1. INTRODUCTION

The Navy Standard Surf Model (NSSM) has been used throughout the Fleet since it was first developed by Earle (1989). It is part of the Geophysical Fleet Mission Program Library (GFMPL) and the Oceanographic and Meteorological Master Library (OAML). Prior to its development, forecasting techniques were based on manual methods that did not adequately consider local shallow water effects. At present, the NSSM is the primary software for operational surf forecasting. It is also used for systems development and surf climate descriptions. SURF 3.2 is the most recent upgrade of the NSSM series. The model is denoted SURF in this report.

Surf zone characteristics influence decisions during nearshore and amphibious military operations. To describe the surf, the Navy uses several parameters such as those defined in the *Joint Surf Manual* (Commander, Naval Surface Force, Pacific and Commander Naval Surface Force, Atlantic, 1987). These parameters include the height of the highest one-third of the breaking waves, the time between successive breaking waves, the angle between breaking waves and the beach, the type of breaking waves, and the maximum longshore current velocity. A dimensionless number called the Modified Surf Index (MSI) provides a measure of overall surf conditions. Other influences on nearshore operations (U.S. Naval Oceanographic Office, 1969) are surf zone width, wave length in the surf zone, the average depth of water at the point of breaking, the direction from which sea or swell approaches the coast, the speed of breakers, and the steepness of breakers. These other influences can be estimated with the surf model.

In this report, we focus on the accuracy of wave height and longshore current from SURF. The validation of SURF using the laboratory data of Visser (1991) and Reniers and Battjes (1997) is documented and the field comparison from Hsu et al. (2000) is summarized. Wave refraction and shoaling are validated using a linear wave model. At the request of NAVOCEANO, the model was run using a very large set of bathymetric profiles from the Beach Survey Chart (BSC) database. This series of runs tested the operation of the model and its error messaging over a wide range of beach profiles, including profiles with very few points.

2. MODEL DESCRIPTION

SURF is a parametric one-dimensional model based on the work of Thornton and Guza (1983, 1986), who developed models for random wave processes including a wave height transformation model and a longshore current model. These models contain both numerical and analytical solutions that provide cross-shore profiles of wave height, and longshore current velocity. Because SURF is one-dimensional, certain approximations are made: (1) straight and parallel bottom contours, (2) wave heights are Rayleigh distributed, and (3) directional wave spectra are narrow-banded in frequency and direction.

SURF requires the following information to perform calculations: (1) a depth profile; (2) wind speed and direction, (3) wave conditions defined by wave parameters, a directional wave spectrum, or a precomputed wave transformation coefficient (also called a transfer function) for a complicated bathymetry. The profile information can be accessed from external data files or generated internally based on reasonable assumptions about the sand size. The user can choose from an internally generated wave spectrum or an external wave spectrum file. If the internally generated spectrum is selected, a modified Pierson-Moskowitz (1964) wave spectrum is calculated from the sea and swell conditions defined by the user in the surf model input file.

SURF outputs are the following: (1) forecasts in the SURFCST/SUROB format from the *Joint Surf Manual*; (2) MSI numbers; (3) cross-shore profiles of water depth, wave heights, wave lengths, percent breaking waves and longshore currents at regularly spaced intervals throughout the surf zone; and (4) a shoaled and refracted directional wave spectrum at a user-specified depth.

2.1 Improvements Leading to SURF 3.2

Several major changes in SURF 3.0 resulted in the upgrade to SURF 3.1. The first and most significant change was the incorporation of a depth-dependent bottom friction function based on the work of Hsu et al. (2000). This change provides a realistic distribution of the longshore current across the surf zone. Second, SURF 3.0 had a tendency to end abruptly without an error message when processing depth input files with sparse data. To overcome the effect of sparse data, several error-checking routines were introduced. Third, the routine that bilinearly interpolates shoaling and refraction matrices was corrected. Fourth, the format of the input file to SURF was changed significantly and the number of input parameters was reduced.

The computational integrity of NSSM was evaluated using nearshore depth profiles from the NAVOCEANO BSC database. Depth profiles were extracted from this database and reformatted into SURF-readable files. Profiles with a deepest depth shallower than 3 meters were culled, leaving 568 profiles. No irregular or unusual profiles were culled. The model was run using four sets of wind, wave, and tide conditions shown in Table 1 for each profile.

Table 1— Input Wave Conditions for Beach Survey Chart Tests

Set	H_{sea} (feet)	T_{sea} (s)	θ_{sea} (deg)	H_{swell} (feet)	T_{swell} (s)	θ_{swell} (deg)	wind speed (knots)	wind direction (deg)	tide (feet)
1	3	5	45	0	--	--	10	30	0
2	3	5	45	0	--	--	10	30	-3
3	0	--	--	3	12	30	10	30	0
4	0	--	--	3	12	30	10	30	-3

H_{sea} is the significant wave height of the locally generated wind waves; T_{sea} is the peak period of the locally generated wind waves; θ_{sea} is the peak direction of the locally generated wind waves in degrees from shore normal; H_{swell} is the significant wave height of swell waves in feet; T_{swell} is the peak period of swell waves in seconds; θ_{sea} is the peak direction of swell waves in degrees from shore normal.

The original series of 568 profiles × 4 runs per profile = 2272 runs produced 2159 surf model forecasts (95 percent) without errors or else with proper diagnostic error messages. The 113 failed model runs produced crashes with either no error messages or empty output files. One profile caused the machine from which the model was run to freeze. All problems were traced to errors in the interpolation of depth profiles containing fewer than five points. This test indicated a need for improvements in processing the input depth data. Algorithms were integrated into SURF 3.1 to examine the depth profile and give warnings and error messages

based on data sparseness or incompleteness. The model automatically compensates for depth profiles that do not extend to the shoreline. If a depth profile does not extend far enough shoreward, errors can occur when tides are specified. The addition or subtraction of water depths to include the tide can cause the water levels to extend beyond the length of the original depth data. SURF 3.1 considers this possibility and inserts a zero depth in each profile. The changes to the depth file handling in SURF 3.1 were tested using the same BSC profiles and four sets of conditions. For each of the 2272 runs, the revised software produced either a complete output file or an appropriate diagnostic message, making it more robust than earlier versions.

Shortly after completing SURF 3.1, typographical errors in the look-up table used for MSI calculations were discovered. In the process of making the corrections to the look-up tables, seven other refinements to the model were also included:

1. We further improved the manner in which wave energy is refracted and shoaled using an input transfer function file. The transfer function reading and regridding subroutine is revised to eliminate the errors introduced by the earlier cubic-spline and the 359-0 degree crossover.
2. At the request of the Naval Oceanographic Office, the input parameter *dstart* was eliminated. This parameter governed the depth at which model integration begins. This depth is now based on the given depth profile, the depth associated with input wave information and the depth of incipient wave breaking.
3. A longer slope computation length is implemented based on wave length and surf zone width. Previous short length leads to unrealistic percentage of surging breakers.
4. The initial breaker angle at the wave spectrum depth is refined to accept wave input angle larger than 45 degrees.
5. Breaker angle was added as an additional output.
6. Numerous comments and diagnostic messages are added.
7. Many improvements are made to streamline the code.

2.2 Wave Model in SURF

As waves approach the coast, the frictional effect of the sea floor on the organized orbital motion of water particles causes waves to break or spill. The flows of spilling breakers can be separated into an upper layer of turbulent energy and a lower layer of organized oscillatory wave motion. The region of turbulent water above the wave is the surface roller. The original idea of defining the wave structure as a two-layer system was introduced by Longuet-Higgins and Turner (1974) (see also Svendsen (1984a,b)). SURF incorporates the roller model of Lippman et al. (1996) that produces results consistent with measurements from both a planar and a barred beach. The energy associated with each layer is used to shoal the incoming waves and drive the longshore current. The energy per unit surface area in a nonbreaking wave is calculated as

$$E_w = \frac{1}{8} \rho g H_{rms}^2 , \tag{1}$$

where ρ is water density and g is the acceleration due to gravity. H_{rms} is the root-mean-square (RMS) wave height. The energy per unit area associated with a roller is given as

$$E_r = \frac{1}{8} \rho c f \frac{H_b^3}{h \tan \beta} , \tag{2}$$

where c is the phase speed of the wave, f is the zero crossing frequency, H_b is the height of the wave at breaking, h is water depth, and β is the angle the roller makes with the body of the wave. A default value of 5 degrees is used for the roller angle.

2.3 Energy Dissipation Model

As a wave propagates across the surf zone, its energy is dissipated due to bottom friction, wave breaking, turbulence, and wave-current interaction. The energy dissipation is given by the energy flux equation

$$\frac{\partial(E_w c_g \cos \theta)}{\partial x} = - < \varepsilon_b > ,$$

(3)

where E_w is the wave energy, c_g is the wave group velocity, and θ is the wave direction relative to shore normal *(x positive offshore)*. The right-hand side of the above equation, $<\varepsilon_b>$, is the ensemble averaged dissipation function. Thornton and Guza (1983) modeled this dissipation function as

$$< \varepsilon_b > = \frac{1}{4} \rho g f \frac{B^3}{h} \int H^3 p_b(H) dH ,$$

(4)

where B is an empirical coefficient, and $p_b(H)$ is the probability distribution for breaking waves described by

$$p_b(H) = W(H)p(H) ,$$

(5)

where $p(H)$ is a Rayleigh Distribution of wave heights and $W(H)$ is a weighting function resulting in a weighted Rayleigh distribution. Several weighting functions have been constructed by various authors. The weighting function applied in SURF, developed by Thornton and Guza (1986), is given as

$$W(H) = \left[\frac{H_{rms}}{\gamma h} \right]^4 \left(1 - e^{-\left[\frac{H}{\gamma h} \right]^2} \right) ,$$

(6)

where γ is an empirical factor determined from field data to be 0.42, h is the water depth, and H is the wave height. If wave roller energy is considered in the model, the modified energy flux equation is defined as

$$\frac{\partial(E_w c_g \cos \theta)}{\partial x} + \frac{\partial(E_r c \cos \theta)}{\partial x} = - < \varepsilon_r >$$

(7)

and the dissipation becomes a function of the roller term. Equation (8) is solved using a numerical forward difference and convergence scheme to determine wave and roller energy along with H_{rms} values at each point.

$$< \varepsilon_r > = \frac{1}{4} \rho g f \frac{H_b^3}{h} \cos \sigma \int H^3 p_b(H) dH$$

(8)

2.4 Longshore Current Model

When waves enter the surf zone at an angle, the shore-parallel component of momentum drives a current along the shore. This longshore current can be a significant force inside the surf zone. Calculation of the current velocity is based on radiation stress theory (see Longuet-Higgins 1970a, 1970b). A general form of the longshore momentum equation is

$$\tau_y^h + \rho \frac{d}{dx}\left(\mu h \frac{dV}{dx} \right) - <\tau_y^b> + \tau_y^w = 0 \quad,$$
(9)

where ρ is the water density, h is the water depth, and V is the longshore current. The first term on the left-hand side is the radiation stress in the longshore direction exerted by waves on the water given by

$$\tau_y^h = <\varepsilon_b> \frac{\sin\theta}{c} \quad,$$
(10)

where ε_b is the dissipation function defined in the previous section, c is wave phase speed, and θ is the angle of wave approach with respect to x. The second term is the horizontal mixing. The horizontal eddy viscosity μ is modeled after Battjes (1975):

$$\mu = Mh\left(\frac{\varepsilon_b}{\rho} \right)^{\frac{1}{3}} \quad,$$
(11)

where M is an empirical constant equal to 1.0. The third term is the mean stress due to bottom friction given by

$$\tau_y^b = \rho\, c_f\, uV \quad,$$
(12)

where c_f is the bottom friction coefficient, u is the magnitude of the near-bottom horizontal wave orbital velocity, and V is the longshore current. Linear wave theory defines the near-bottom wave-induced orbital velocity as

$$u = \frac{\pi H}{T \sinh(kh)} \quad,$$
(13)

where H is the wave height, T is the wave period, and k is the wave number that can be calculated using the dispersion relation

$$\sigma^2 = g\, k\, \tanh(k\, h) \quad,$$
(14)

where σ is the radian wave frequency and g is gravity. The longshore current equation is solved using a finite difference approach after wave heights, water depths, and wave dissipation values are calculated at each cross-shore grid point in the surf zone.

The depth-dependent bottom friction coefficient function is defined as

$$
c_f(x) = \begin{cases} 0.003 & ; \ x \geq \dfrac{X_b}{2} \\[2em] 0.003\left(\dfrac{h\dfrac{X_b}{2}}{h(x)}\right) & ; x < \dfrac{X_b}{2} \end{cases} \ ,
\tag{15}
$$

where x is the offshore distance, h is the local water depth, and X_b is the distance from the shoreline to the location where 10 percent of the waves are breaking.

3. VALIDATION OF WAVE HEIGHT AND LONGSHORE CURRENT

SURF has been extensively validated with regard to wave height and longshore current by Hsu et al. (1997, 2000). Model performances using the laboratory data of Visser (1991) on a flat beach, and of Reniers and Battjes (1997) on a barred beach are presented. The surf zone width, an important surf output and modeling parameter, has been validated by Mettlach et al. (1999) and is not included here.

3.1 Laboratory Tests

The work of Visser (1991) and Reniers and Battjes (1997) provide important data sets in examining phenomena that, in the field, cannot be easily isolated from other processes. In this section, wave height and longshore current from a modified version of SURF are compared to laboratory measurements. It is noted that the model calculation interval and termination depth were altered from the standard settings of 2 ft and 0.5 ft, respectively, to 0.1 ft and 0 ft, respectively. This was, of course, necessary to achieve profiles covering the complete range of measurement depths.

3.1.1 Visser

Visser (1991) measured longshore currents in a wave-basin using a pump-driven recirculation method to simulate an open coast and produced uniform longshore currents. All eight cases presented in Visser (1991) are used in this report. A summary of the model initial conditions for the eight cases is given in Table 2. There are two bottom slopes and two bottom types. Note that cases 4 and 7 and cases 5 and 8 are identical except for bottom type. The difference in longshore current magnitudes between concrete and gravel surfaces highlights the importance of using the correct bottom friction coefficient.

Table 2 — Initial Wave Conditions and Bottom Characteristics in Visser (1991)

Case	H_o (m)	T_p (s)	θ_p (degrees)	Bottom Slope	Bottom Type
1	.07	2.01	31.1	.101	Smooth Concrete
2	.09	1.00	30.5	.101	Smooth Concrete
3	.09	1.00	15.4	.050	Smooth Concrete
4	.08	1.02	15.4	.050	Smooth Concrete
5	.07	1.85	15.4	.050	Smooth Concrete
6	.06	0.70	15.4	.050	Smooth Concrete
7	.08	1.02	15.4	.050	Gravel
8	.07	1.85	15.4	.050	Gravel

Cross-shore distributions of wave height, estimated percent wave breaking, and longshore current predictions and measurements are given in Figs. 1 through 6. Note that cases 4 and 7 and cases 5 and 8 are combined in Figs. 4 and 5, respectively. In each plot, the solid curves are output from SURF with the variable bottom friction formulation. The dotted curve in the lower panel of each plot gives the longshore current from the SURF 3.0 with constant bottom friction. It is noted that the change in bottom friction does not affect wave height or percent breaker calculations so the wave height and percent breaker profiles from both versions of the model are not shown on these plots.

The model wave heights do not compare as well as they have with field studies. In addition, in each case there is a sharp rise in measured height near the breakpoint. This feature is not produced by the model. These differences can be attributed to many reasons. The wave model in SURF is based on the work of Thornton and Guza (1983) in which the energy dissipation model is formulated for the spilling breakers as propagating bores. In Visser's paper, it is stated that all breakers are of the plunging type except case 6, which are of the transitional spilling/plunging type. In addition, the field derived empirical constants may not be appropriate for use with the regular waves in Visser's experiment as a common scaling problem. SURF also assumes that the predicted waves are random and follow a Rayleigh distribution, whereas the laboratory tests were conducted for regular waves. All of these factors can contribute to the differences.

In longshore current comparisons, it is apparent that SURF produces more accurate longshore current estimates than the earlier version. Another major problem of earlier estimates is that the peak current often occurs near the end of the beach, which is clearly not acceptable, as illustrated in Figs. 1, 2, and 3. SURF now produces a peak near the half of the surf zone consistent with the measurements. It is very encouraging to see SURF results fall in between smooth concrete and coarse gravel surfaces as illustrated in Figs. 4 and 5. The empirical constants for horizontal diffusion and bottom friction formulation of SURF are calibrated from field data taken from sandy bottoms. The fact that SURF results fall in between these two surfaces indicates that our bottom friction formulation and calibrations are properly conducted.
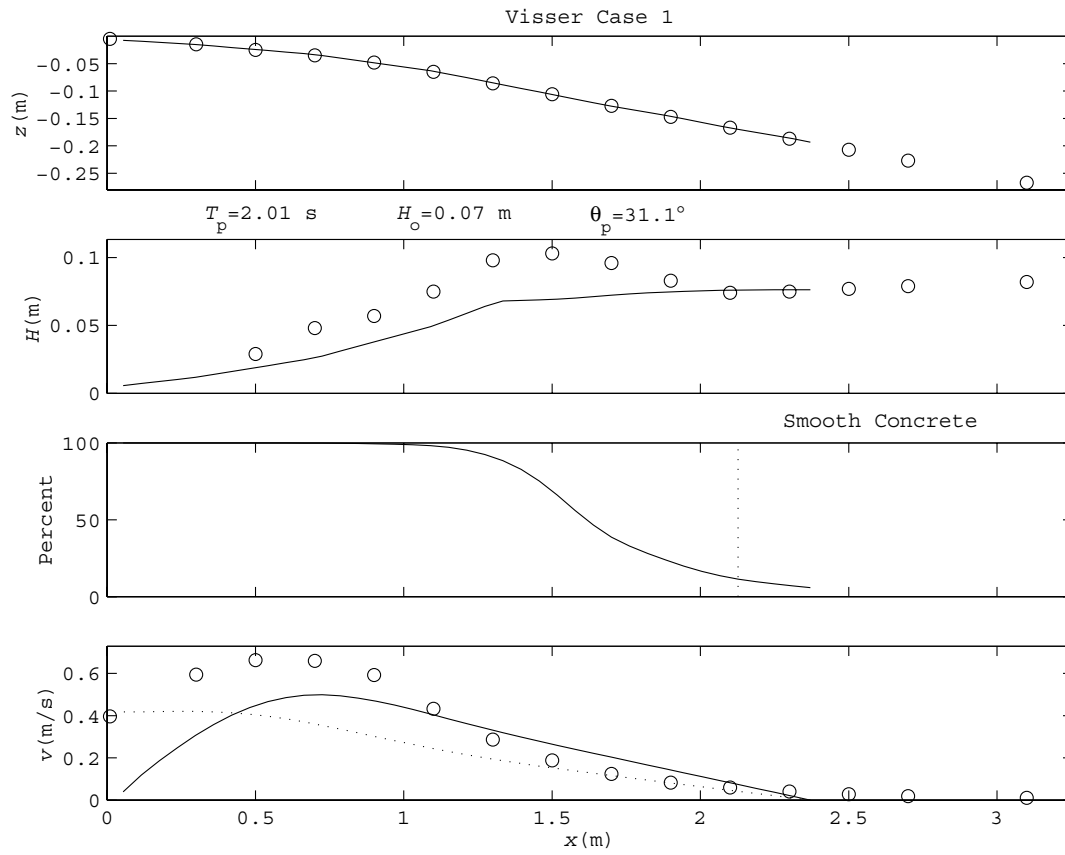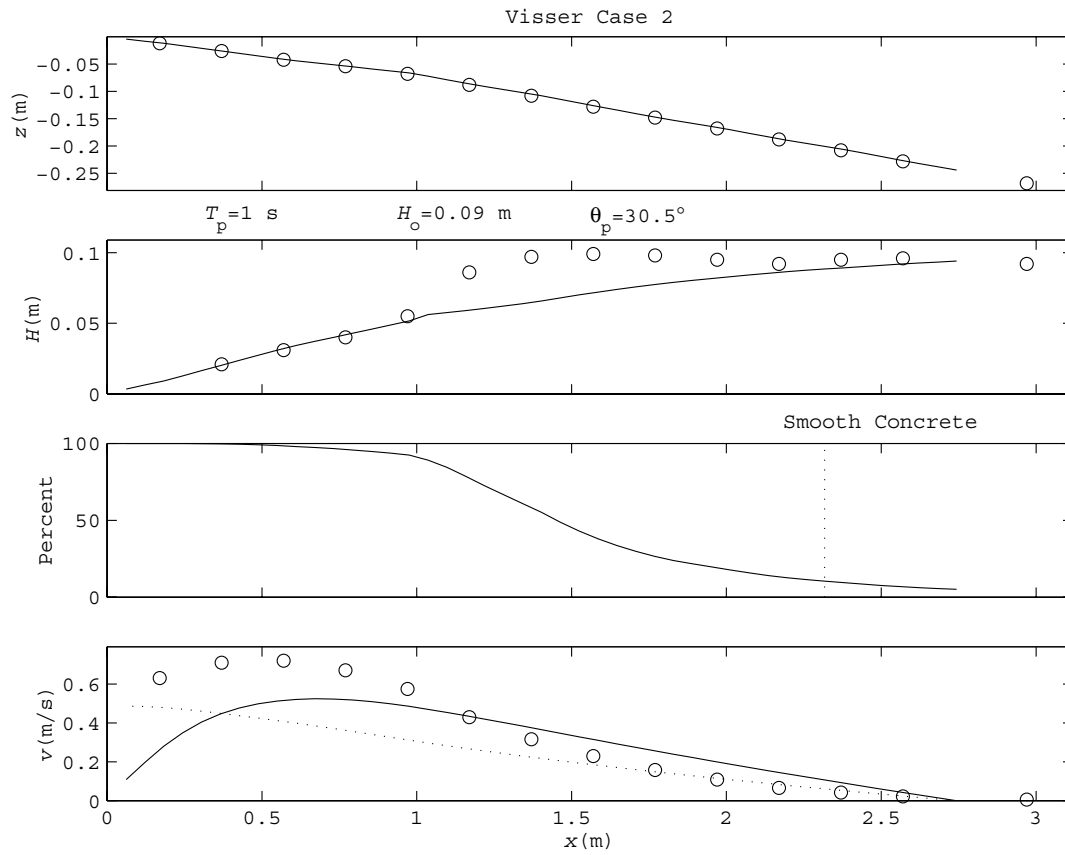
Fig. 1 — Visser Case 1. Top panel: depth *z* from model (solid line) and measured ("o"). Second panel: RMS wave height *H* from model (solid line) and measured ("o"). Third panel: percentage of breaking or broken waves estimated by model. The dotted vertical line is the beginning of the offshore point where the percent of breaking is > 10 percent, which defines the beginning of the surf zone. Bottom panel: longshore current *v* from SURF 3.0 (dotted) and SURF with improved longshore current (solid). Measured *v* is denoted by "o." Wave conditions used to initialize the model and the bottom material are noted.
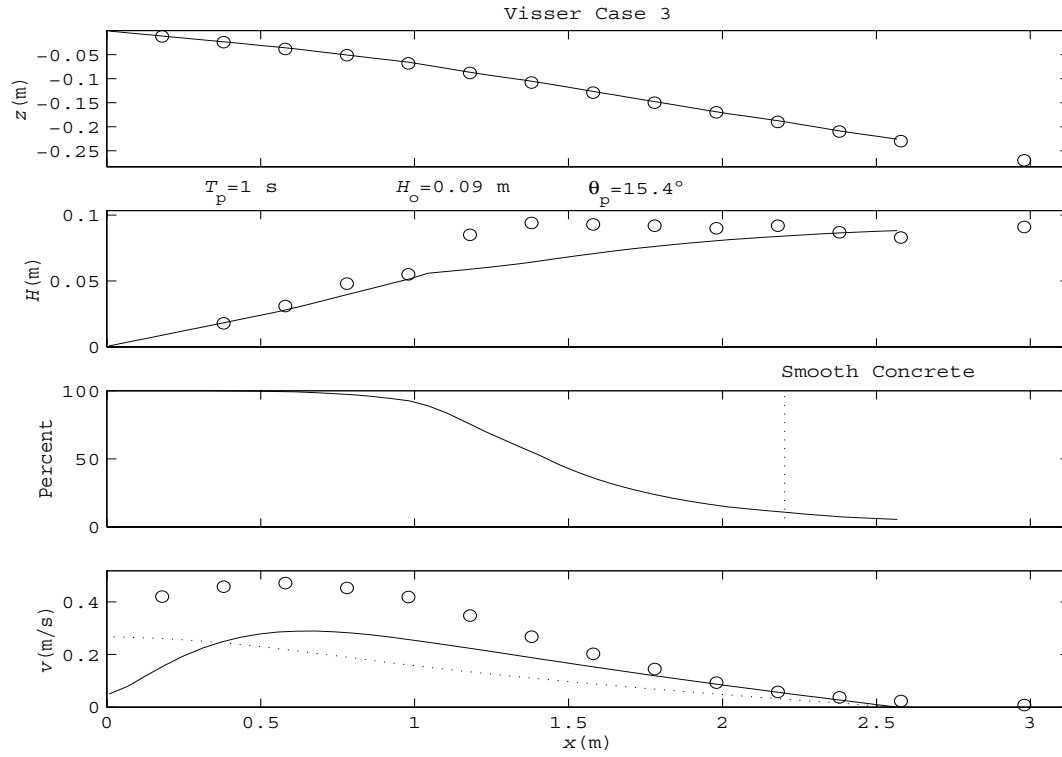
Fig. 2 — Visser Case 2. Top panel: depth z from model (solid line) and measured ("o"). Second panel: RMS wave height H from model (solid line) and measured ("o"). Third panel: percentage of breaking or broken waves estimated by model. The dotted vertical line is the starting point where the percent of breaking is > 10 percent, which defines the beginning of the surf zone. Bottom panel: longshore current v from SURF 3.0 (dotted) and SURF with improved longshore current (solid). Measured v is denoted by "o." Wave conditions used to initialize the model and the bottom material are noted.
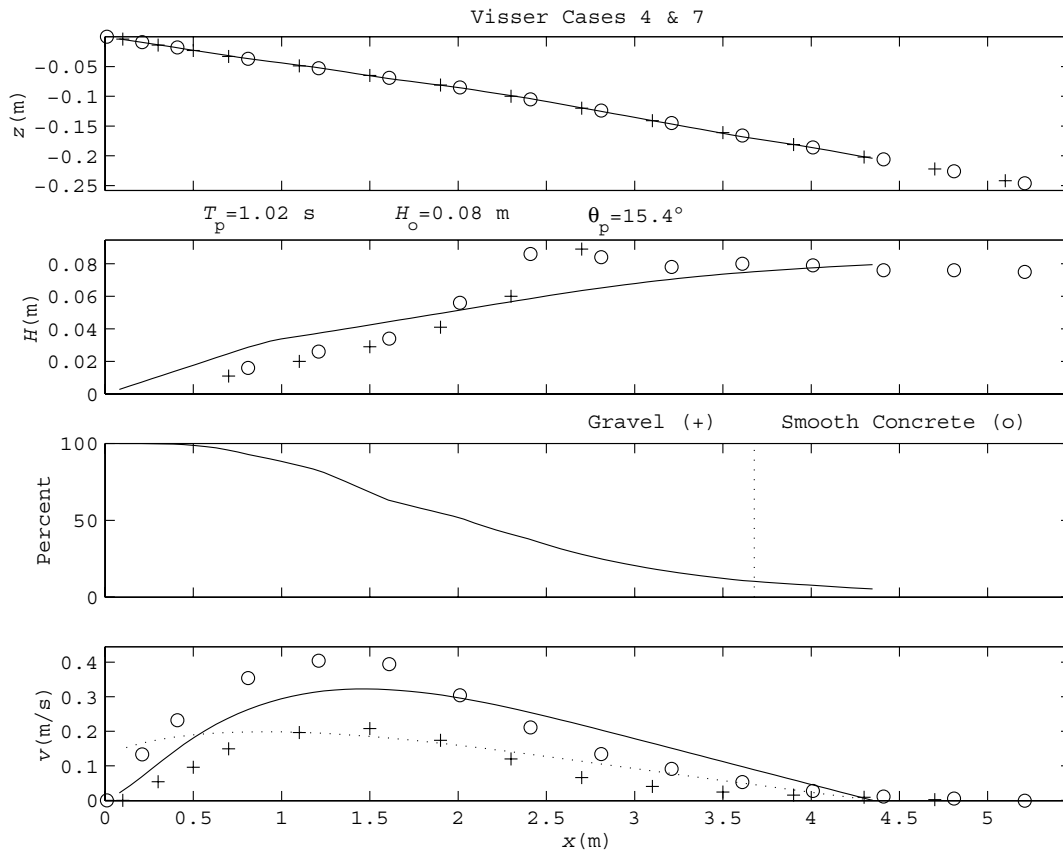
Fig. 3 — Visser Case 3. Top panel: depth *z* from model (solid line) and measured ("o"). Second panel: RMS wave height *H* from model (solid line) and measured ("o"). Third panel: percentage of breaking or broken waves estimated by model. The dotted vertical line is the starting point where the percent of breaking is > 10 percent, which defines the beginning of the surf zone. Bottom panel: longshore current *v* from SURF 3.0 (dotted) and SURF with improved longshore current (solid). Measured *v* is denoted by "o." Wave conditions used to initialize the model and the bottom material are noted.
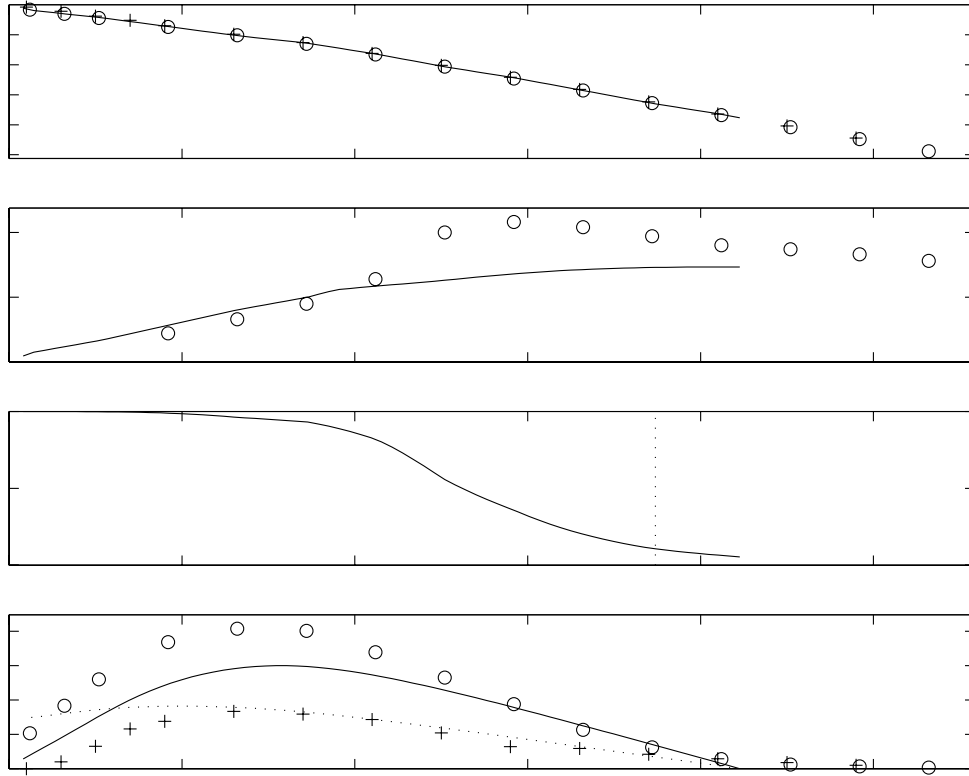
Fig. 4 — Visser Cases 4 and 7. Top panel: depth z from model (solid line) and measured ("o" and "+"). Second panel: RMS wave height H from model (solid line) and measured ("o" and "+"). Third panel: percentage of breaking or broken waves estimated by model. The dotted vertical line is the starting point where the percent of breaking is > 10 percent, which defines the beginning of the surf zone. Bottom panel: longshore current v from SURF 3.0 (dotted) and SURF with improved longshore current (solid). Measured v is denoted by "o" and "+". Wave conditions used to initialize the model and the bottom material are noted.

Fig. 5 — Visser Cases 5 and 8. Top panel: depth *z* from model (solid line) and measured ("o" and "+"). Second panel: RMS wave height *H* from model (solid line) and measured ("o" and "+"). Third panel: percentage of breaking or broken waves estimated by model. The dotted vertical line is the starting point where the percent of breaking is > 10 percent, which defines the beginning of the surf zone. Bottom panel: longshore current *v* from SURF 3.0 (dotted) and SURF with improved longshore current (solid). Measured *v* is denoted by "o" and "+". Wave conditions used to initialize model and bottom material are noted.
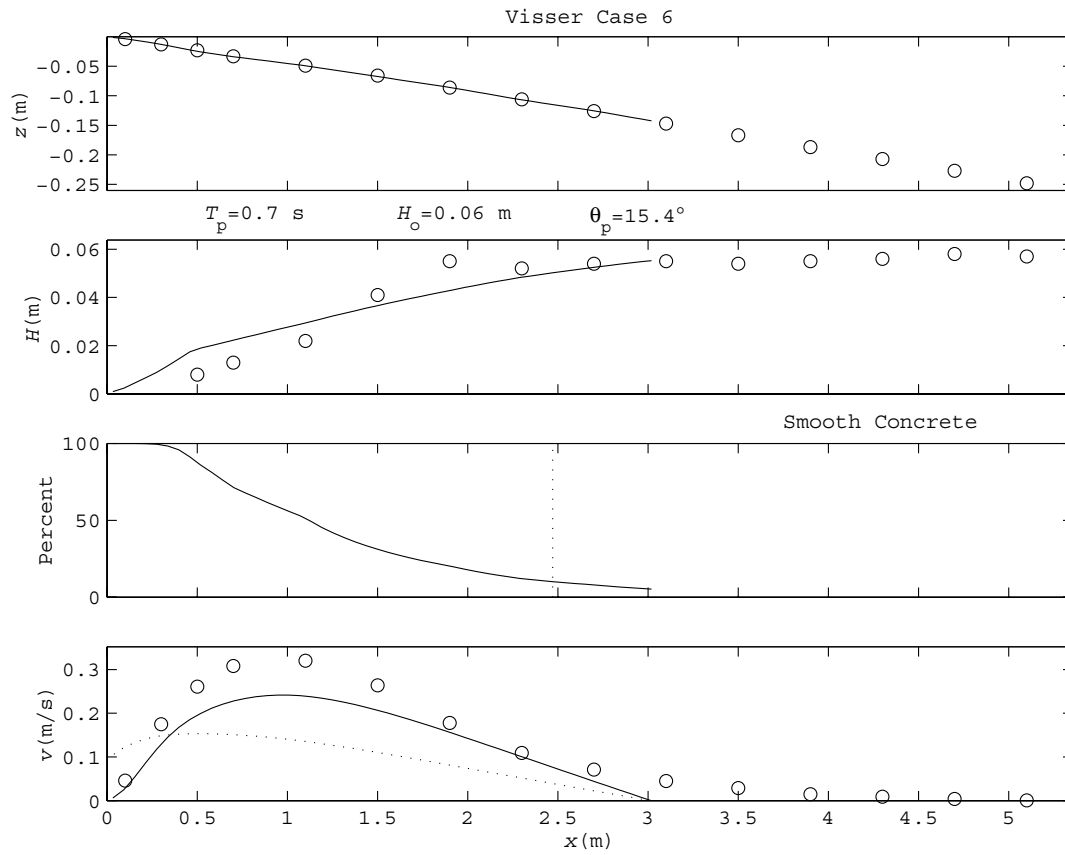
Fig. 6 — Visser Case 6. Top panel: depth z from model (solid line) and measured ("o"). Second panel: RMS wave height H from model (solid line) and measured ("o"). Third panel: percentage of breaking or broken waves estimated by model. The dotted vertical line is the starting point where the percent of breaking is > 10 percent, which defines the beginning of the surf zone. Bottom panel: longshore current v from SURF 3.0 (dotted) and SURF with improved longshore current (solid). Measured v denoted by "o." Wave conditions used to initialize model and bottom material are noted.

3.1.2 Reniers and Battjes

The Reniers and Battjes (1997) study offers new data set including barred beach and random wave input. An important characteristic of the longshore current measurements acquired at a barred beach, Duck, NC, is that the peak in longshore current is typically not located over the crest of the bar but, rather, over the trough shoreward of the bar. Several researchers have attempted to explain this apparent contradiction to radiation stress theory with new bed stress models, lateral mixing models and roller models.

Reniers and Battjes (1997) examined the location of the longshore current peak using a large wave-basin at the Delft University of Technology, The Netherlands. An alongshore bar was constructed in the wave-basin. Water was recirculated to simulate open coast longshore uniformity. Data from three cases by Reniers and Battjes (1997) were used for comparison. Table 3 summarizes the cases.

Table 3 — Initial Wave Conditions and Characteristics Given for Three Cases in Reniers and Battjes (1997)

Case	H_o (m)	T_p (s)	θ_p (degrees)	Test Description
SA243	0.08	1.0	30	Regular waves; barred beach
SA337	0.10	1.0	30	Regular waves; barred beach
SO014	0.07	1.2	30	Random waves; barred beach

The cases are summarized in Figs. 7 through 9 with the same notation as used in the Visser figures. For the random waves case in Fig. 9, the surf zone is wider and longshore current profile is smoother as expected due to varying breaking locations. The wave heights from SURF generally agree better than do those in Visser's cases. As a result, the agreement of longshore current comparisons is also improved. The predicted locations of peak current are close to the measured peak locations. It is noted that the peak in the measured longshore current is over the crest of the bar and not, as observed at Duck during DELILAH, over the trough shoreward of the crest of the bar.
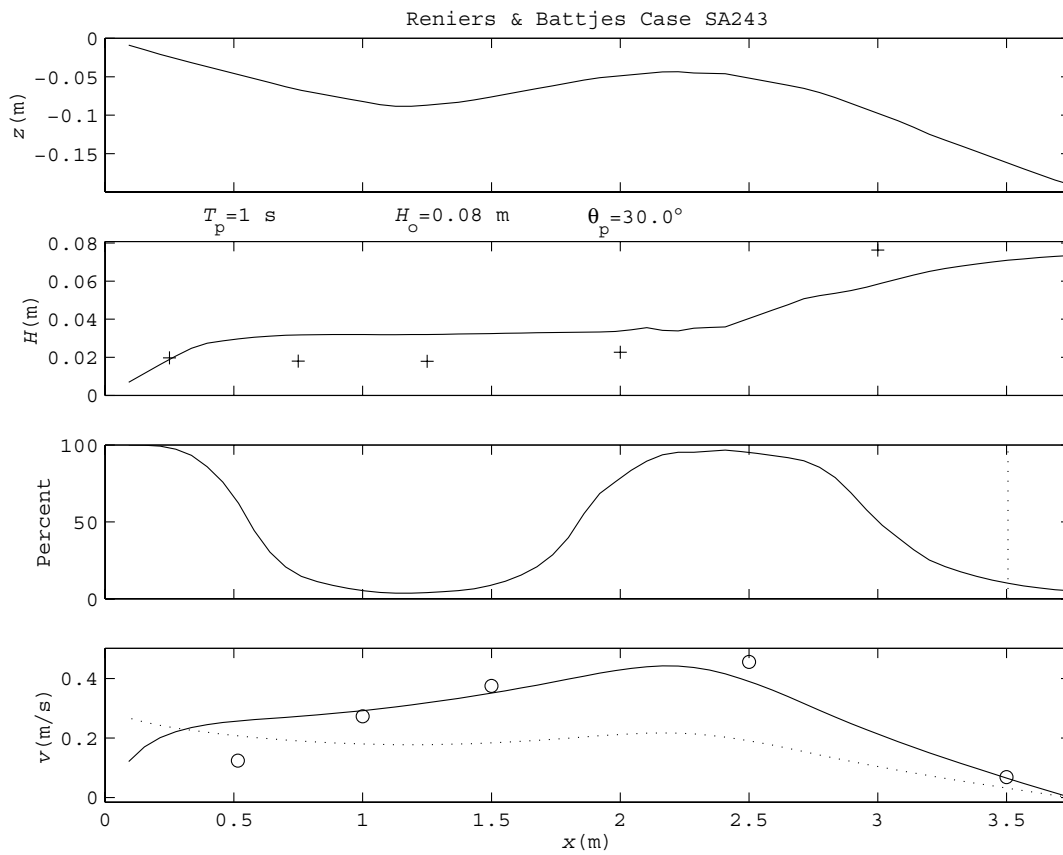
Fig. 7 — Reniers and Battjes Case SA243. Top panel: depth *z* from model. Second panel: RMS wave height *H* from model (solid line) and measured ("+"). Third panel: percentage of breaking or broken waves estimated by model. The dotted vertical line is the starting point where the percent of breaking is > 10 percent, which defines the beginning of the surf zone. Bottom panel: longshore current *v* from SURF 3.0 (dotted) and SURF with improved longshore current (solid). Measured *v* is denoted by "o." Wave conditions used to initialize the model are noted.
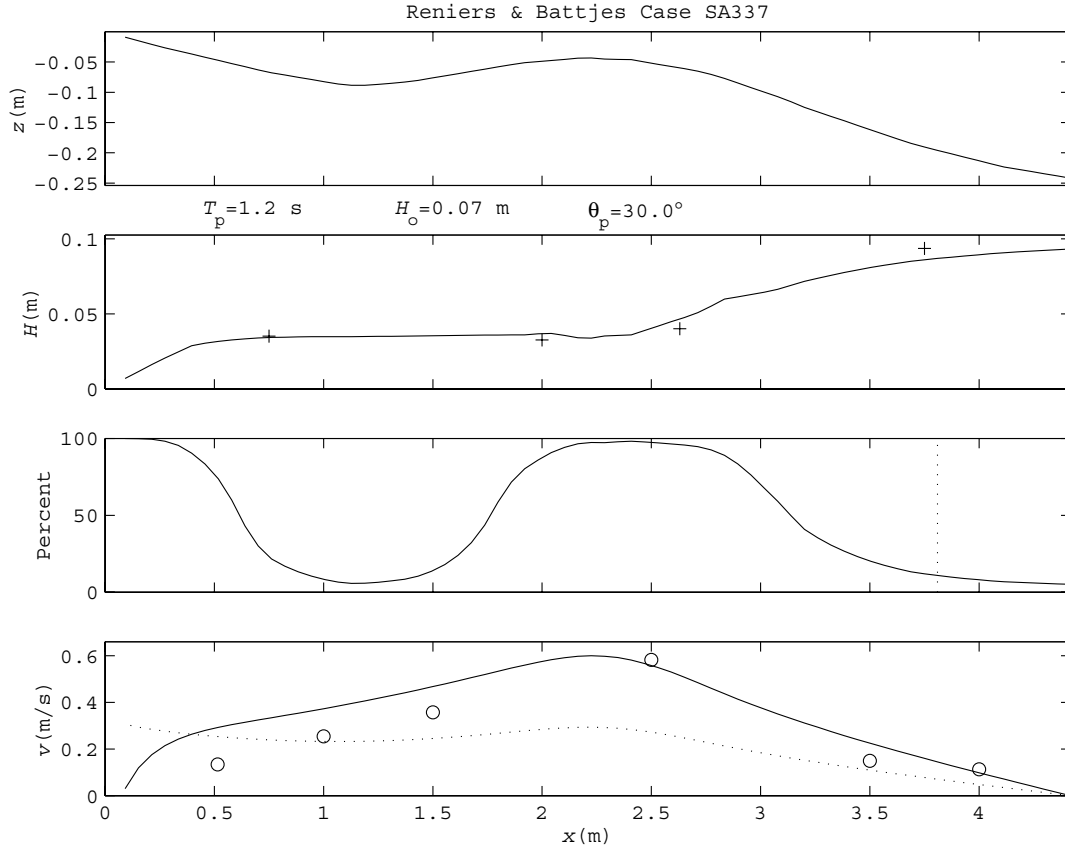
Reniers & Battjes Case SA337

Fig. 8 — Reniers and Battjes Case SA337. Top panel: depth *z* from model. Second panel: RMS wave height *H* from model (solid line) and measured ("+"). Third panel: percentage of breaking or broken waves estimated by model. The dotted vertical line is the starting point where the percent of breaking is > 10 percent, which defines the beginning of the surf zone. Bottom panel: longshore current *v* from SURF 3.0 (dotted) and SURF with improved longshore current (solid). Measured *v* is denoted by "o." Wave conditions used to initialize the model are noted.
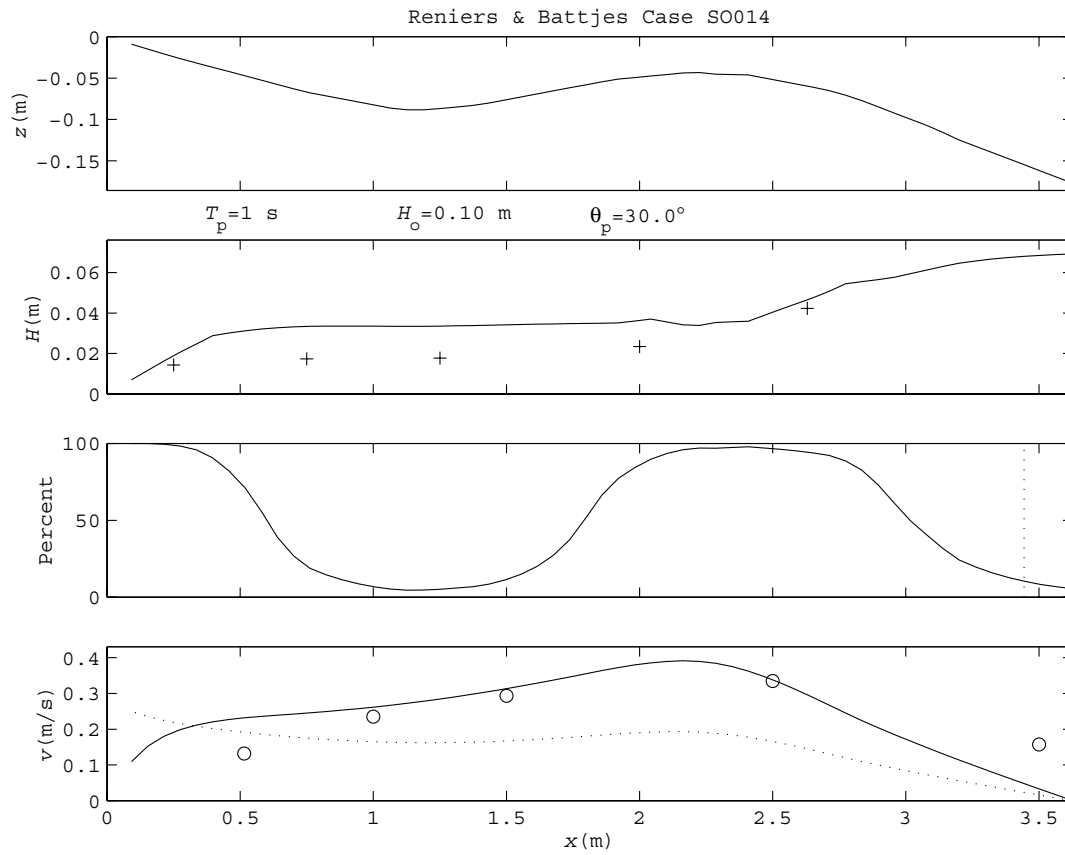
Fig. 9 — Reniers and Battjes Case SO014. Top panel: depth *z* from model. Second panel: RMS wave height *H* from model (solid line) and measured ("+"). Third panel: percentage of breaking or broken waves estimated by model. The dotted vertical line is the starting point where the percent of breaking is > 10 percent, which defines the beginning of the surf zone. Bottom panel: longshore current *v* from SURF 3.0 (dotted) and SURF with improved longshore current (solid). Measured *v* is denoted by "o." Wave conditions used to initialize the model are noted.

3.2 Field Tests

Validation of wave height and longshore current for NSSM using field data acquired during NSTS, DELILAH, and DUCK94 has been reported by Hsu et al. (2000). Four cases from the NSTS experiment at Leadbetter Beach, Santa Barbara, California were used. Seventy-nine cases from a large portion of DELILAH and 144 cases from a large portion of DUCK94 have given a reliable measure of the model's performance over a barred beach. This section summarizes the field comparisons.

There are two major differences between the data from NSTS and those from DELILAH and DUCK94. First, the Leadbetter Beach is largely planar while the beach at Duck generally contains at least one longshore oriented bar. Secondly, the NSTS runs are initialized using an internally generated swell wave spectrum, while the Duck runs were each initialized with the complete directional wave spectrum acquired at the Duck 8-meter-deep array of wave gauges. Communication with Professor Edward Thornton of the Naval Postgraduate School confirmed that on these days the wave conditions at Leadbetter Beach were predominately swell waves, narrowbanded in both frequency and direction. Thus, the assumption that wave conditions were similar to those simulated by the model's internally generated spectrum is valid.

3.2.1 NSTS Leadbetter Beach 1980

Four NSTS cases were presented in Hsu et al. (2000), but only one case is shown here (Fig. 10). Scatter diagrams of measurement-to-model results for all four cases are given for wave height (Fig. 11) and longshore current from the model with the bottom friction improvement (Fig. 12).

The wave heights estimated by the model match measurements to an acceptable level of accuracy with linear correlation of 0.89. The range of errors, mean error, and standard deviation of the errors is quite low. SURF produces good estimates of longshore current and its peak location. The linear correlation coefficient is increased from 0.72 (SURF 3.0) to 0.88 (SURF 3.2). The range of errors is also reduced. The results from the NSTS cases show that SURF performs reasonably well in estimating both wave height and longshore current over a flat or planar beach.
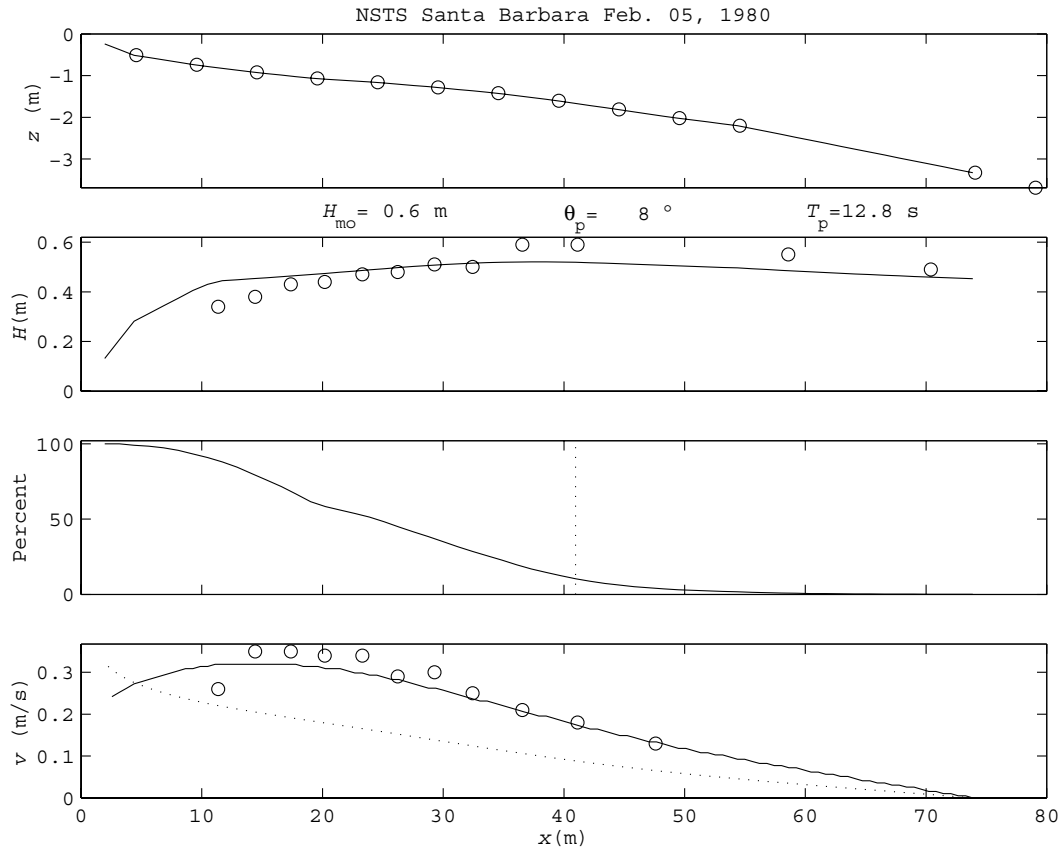
Fig. 10 — NSTS Leadbetter Beach, Santa Barbara, California, February 5, 1980. Top panel: depth *h* = -*z* from model and measured ("o"). Second panel: RMS wave height *H* from model (solid line) and measured ("o"). Third panel: percentage of breaking or broken waves estimated by model. The dotted vertical line is the starting point where the percent of breaking is > 10 percent, which defines the beginning of the surf zone. Bottom panel: longshore current *v* from SURF 3.0 (dashed) and SURF with improved longshore current (solid). Measured *v* is denoted "o." Wave conditions used to initialize the model are noted.
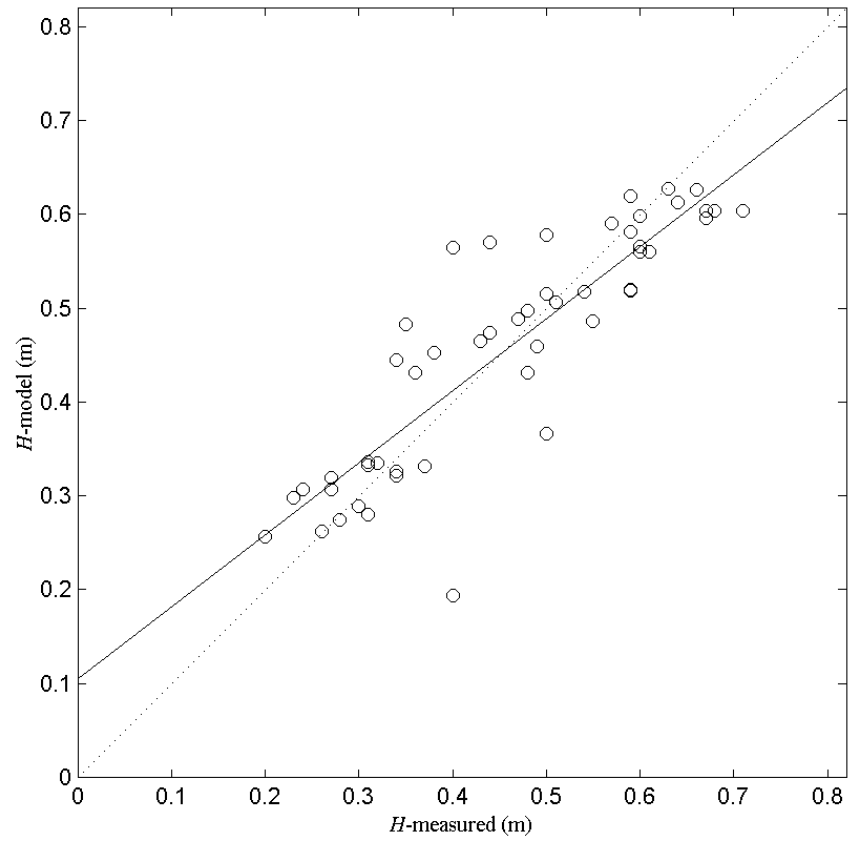
Fig. 11 — Scatter diagram of measured vs modeled RMS wave height. NSTS Leadbetter Beach, Santa Barbara, CA, February 3-6, 1980. The linear correlation coefficient is 0.88 between model estimates and measurements. The standard deviation is 0.1 m.
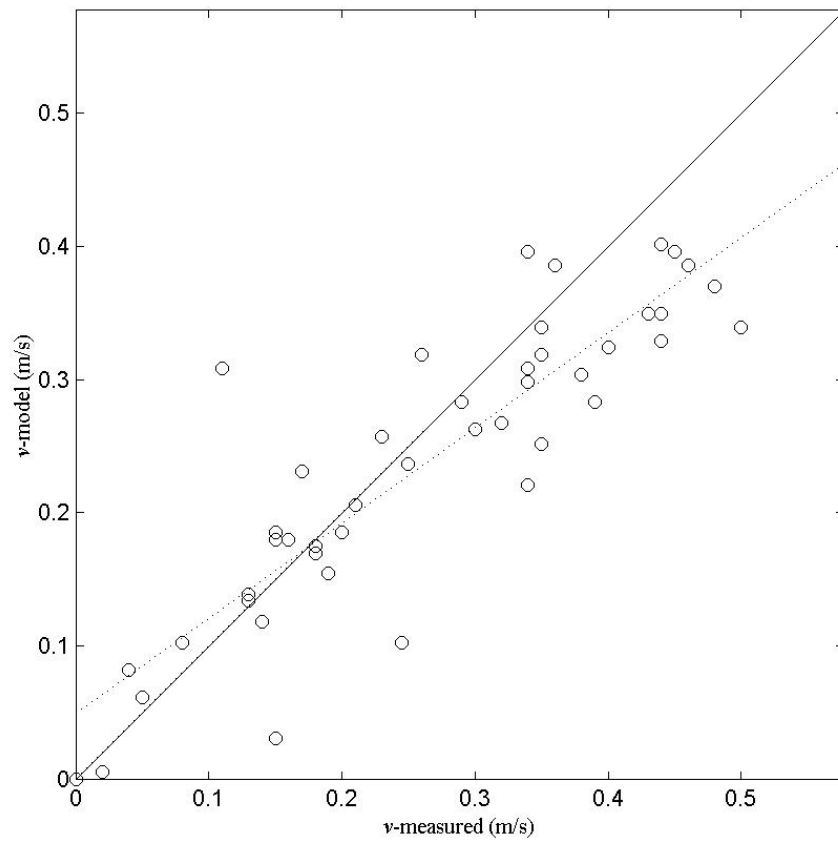
Fig. 12 — Scatter diagram of measured vs SURF (with improvement) longshore current at NSTS Leadbetter Beach, Santa Barbara, CA, February 3-6, 1980. Skill statistics are based on *N* observations and model minus measured differences. The linear correlation coefficient is 0.87 between model estimates and measurements. The standard deviation is 0.1 m/s.

3.2.2 DELILAH and DUCK94

Hsu et al. (2000) give eight sets of profile plots of depth, wave height, percentage of wave breaking, and longshore current from DELILAH and DUCK94. Figures 13 and 14 of this report present single plots from DELILAH and DUCK94, respectively (SURF 3.0 - dashed line; SURF - solid line). Also, Figs. 15 and 16 present, respectively, scatter plots of predicted and measured values of wave height and longshore currents.
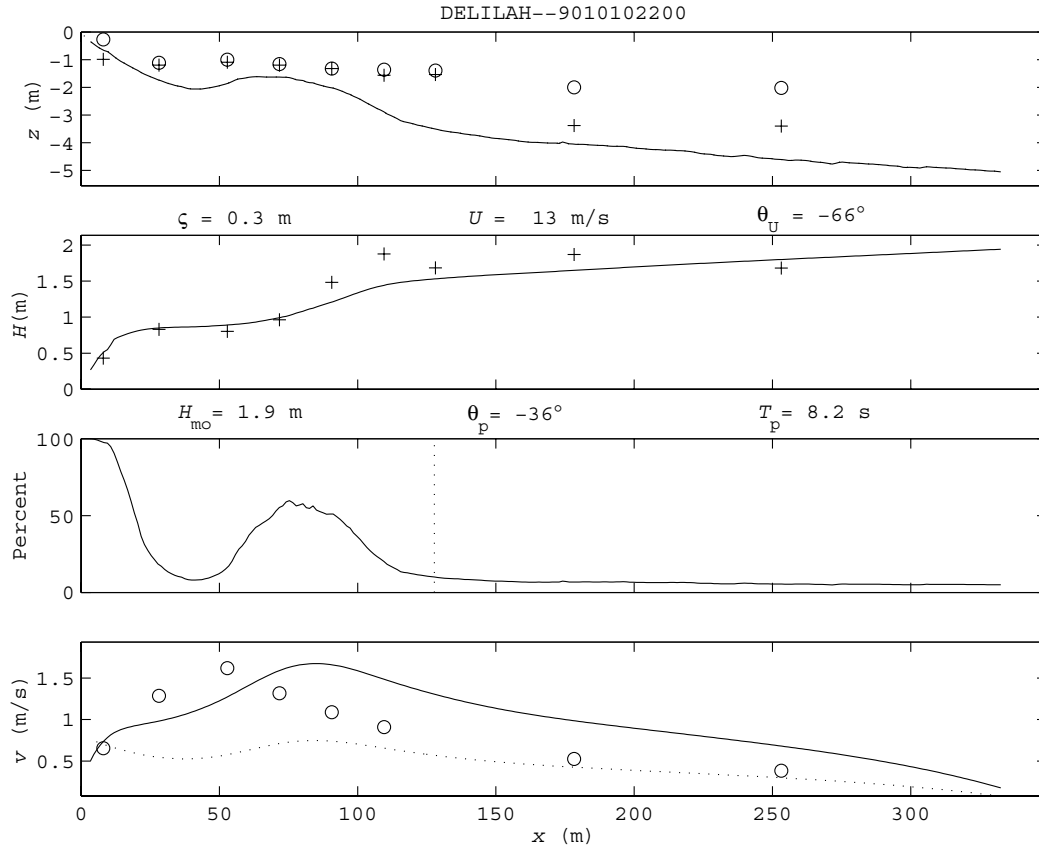

Fig. 13 — DELILAH, 2200 EST October 10, 1990. Top panel: depth $h=-z$ with location of pressure sensors ("+") and current meters ("o"). Second panel: RMS wave height H from model (solid line) and measured ("+"). Third panel: percentage of breaking or broken waves estimated by model. The dotted vertical line is the starting point where the percent of breaking is > 10 percent, which defines the beginning of the surf zone. Bottom panel: longshore current v from SURF 3.0 (dashed) and SURF3.1 with improved longshore current (solid). Measured v is denoted "o." Wind and wave conditions (from the spectrum used to initialize the model) are noted.
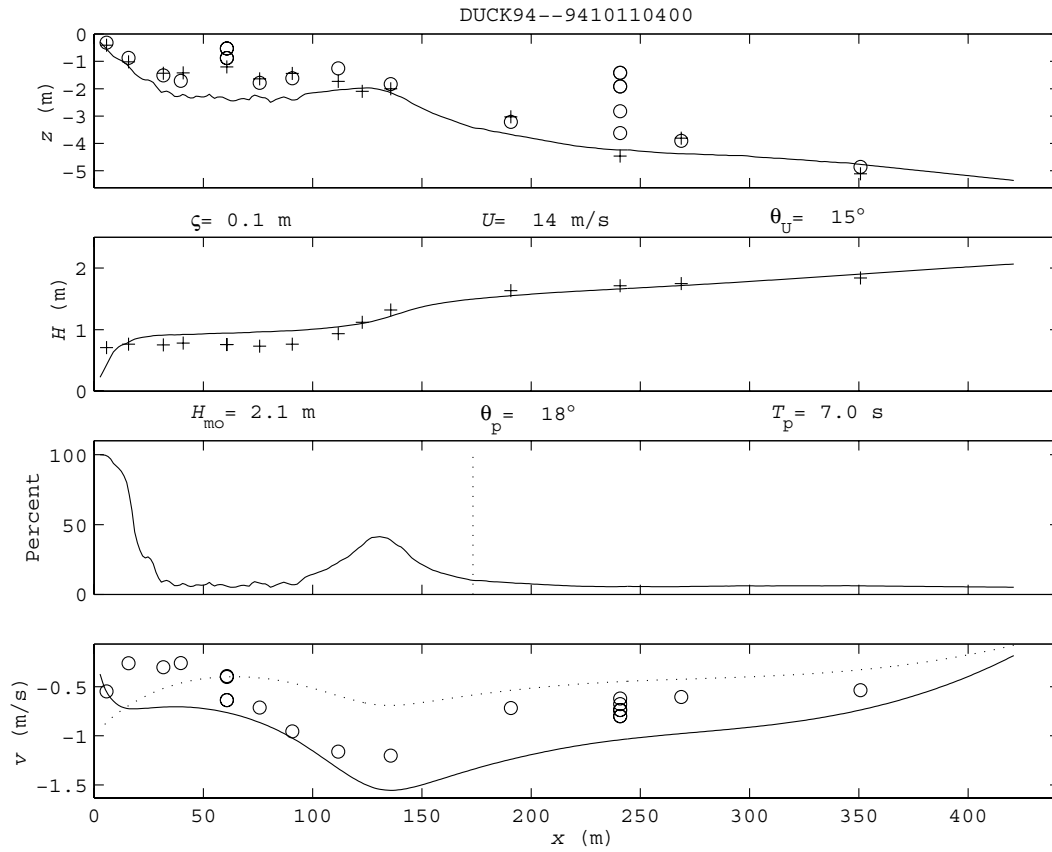
Fig. 14 — DUCK94, 0400 EST October 11, 1994. Top panel: depth $h = -z$ with location of pressure sensors ("+") and current meters ("o"). Second panel: RMS wave height H from model (solid line) and measured ("+"). Third panel: percentage of breaking or broken waves estimated by model. The dotted vertical line is the starting point where the percent of breaking is > 10 percent, which defines the beginning of the surf zone. Bottom panel: longshore current v from SURF 3.0 (dashed) and SURF with improved longshore current (solid). Measured v is denoted "o." Wind and wave conditions (from the spectrum used to initialize the model) are noted.
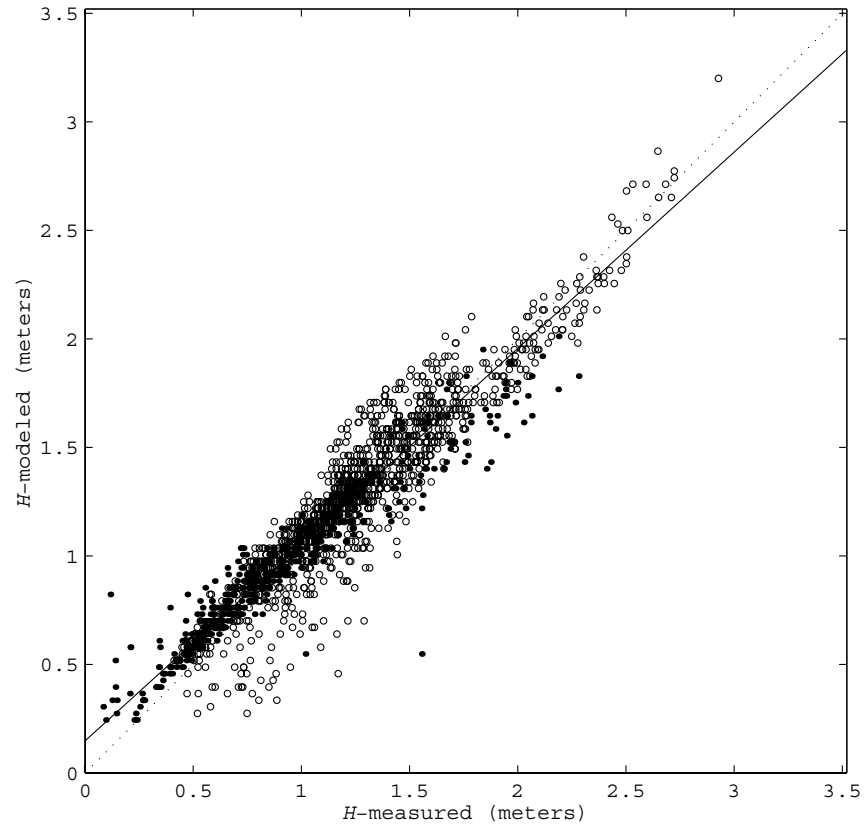
Fig. 15 — Scatter diagram of measured RMS wave heights vs estimates of wave height. Dots denote DELILAH measurements; circles denote DUCK94 measurements. $N = 1796$ observations. The linear correlation coefficient is 0.95 between model estimates and measurements. The standard deviation is 0.15 m.
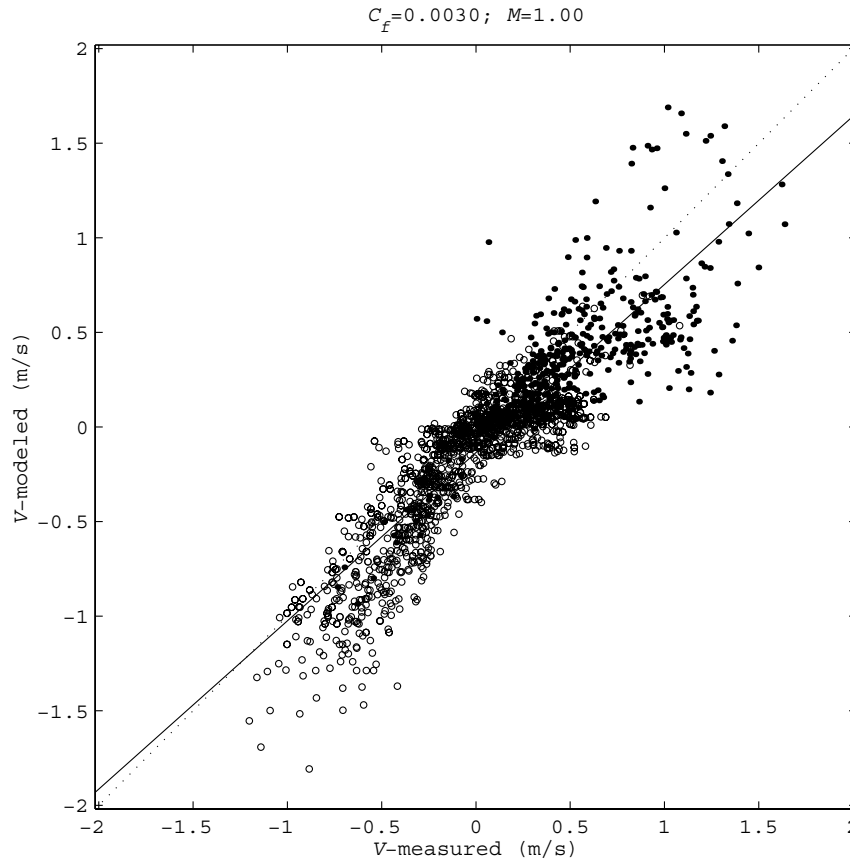
C_f=0.0030; *M*=1.00

Fig. 16 —— Scatter diagram of measured longshore currents vs the corresponding improved SURF estimates of current. Dots denote DELILAH measurements; circles denote DUCK94 measurements. N = 1930 observations. The linear correlation coefficient is 0.88 between model estimates and measurements. The standard deviation is 0.22 m/s.

As shown in Fig. 16, the model produces, on average, quite accurate estimates of wave height in the surf zone. The 1796 observations are matched to model estimates with a correlation of 0.95 and a standard deviation of 0.15 m. For longshore current, the correlation coefficient is 0.88 with a standard deviation of 0.22 m/s. This is an acceptable accuracy for longshore current. The remaining issue is the peak current location at a barred beach as previously mentioned. Inclusion of roller-based parameterization of wave forcing in SURF does not significantly shift the peak toward the trough. Recently, Ruessink et al. (2001) showed that improved peak location can be achieved by using a different roller formulation.

The validation statistics noted on each of the scatter diagrams in this report are summarized in Table 4. It is important to note that the good statistical results contained in Table 4 are derived from surf model runs in which carefully measured scientific field data have been used for model initialization. Surf forecasts for naval operations, based on rough estimates of beach profile and wave conditions, especially for denied areas where reconnaissance observations cannot be made, will, of course, be less accurate than the statistical accuracies given in Table 4.

Table 4 — Summary of Statistics

	R	σ	*M*	*y* (*x* = 0)	*N*
H-NSTS	.88	.1 m	.77	.1 m	51
V-NSTS	.87	.1 m/s	.71	.1 m/s	47
H-DUCK	.95	.15 m	.90	.15 m	1796
V-DUCK	.88	.22 m/s	.89	-.14 m/s	1930

H is root-mean-square wave height and *V* is longshore current speed. NSTS
denotes three cases from Leadbetter Beach. DUCK combined DELILAH
and DUCK94 data sets. Parameter *R* is linear correlation coefficient and σ is
the standard deviation. *M* is the slope of linear regression line and
y(*x* = 0) is *y*-intercept. *N* is the number of measurements.

3.3 Wave Refraction and Shoaling through Transformation Coefficient

SURF can now accept directional spectra from many wave models such as WAM, STWAVE, and SWAN. In addition, it can also accept precomputed transformation coefficients from REFDIF, a shallow water wave refraction and diffraction model. To derive the input parameters for SURF, a given offshore directional spectrum is applied to the corresponding coefficients. The transformation coefficients consist of a matrix of refraction and shoaling coefficients as a function of wave input angle and frequency. Once the transformation coefficients are computed for a domain, they never need to be modified. Nearshore waves can be easily computed at any given point using the coefficients. In those areas, wave models such as STWAVE and SWAN require long computation times because of the required small spatial grid resolution. It should be noted that wind generation is not considered in REFDIF. Therefore, this approach is valid only when additional energy from wind generation is not significant in the computation domain. This is generally true for a limited area regional model under modest wind.

In this section, the SURF computation has been validated using a simulated directional wave spectrum and refraction and shoaling coefficients from a planar beach, i.e., a straight coast with parallel bottom contours. The validation consists of comparing SURF output to the theoretical results from a linear wave theory. The input is a 10-second, 1 ft (0.305 m) wave in a 45-degree direction relative to the beach. Table 5 compares the wave parameters at different depths on a planar. The answers agree well with theoretical results.

Table 5 — Comparison of Wave Parameters Calculated from SURF and Linear Wave Theory on a Planar Beach

	Significant wave height (m)	Average wave direction Degree
Input at 200 m	0.305	45
Output at 8 m SURF	0.274	22.1
Theoretical	0.272	22.3
Output at 5 m SURF	0.289	17.7
Theoretical	0.295	17.9
Output at 2 m SURF	0.366	11.5
Theoretical	0.353	11.6

4. CONCLUSIONS

This report summarizes previous and new validation work conducted for SURF. Wave height has generally been well modeled with an average standard deviation of 0.13 m compared with NSTS, DELILAH, and DUCK94 field data. The average linear correlation coefficient is 0.92. The average standard deviation for longshore current is 0.2 m/s. The average linear correlation coefficient is 0.88. This is a vast improvement over previous versions.

The comparisons with laboratory data are reasonable, but are less accurate than those in field measurements. This can be attributed to many factors such as breaker type and laboratory scaling problems. It is very encouraging to find out that the SURF longshore current result falls between smooth concrete and gravel surfaces. The empirical constants for horizontal diffusion and bottom friction formulation of SURF are calibrated from field data taken from sandy bottoms. The fact that SURF results fall in between these two surfaces indicates that our bottom friction formulation and calibrations are properly conducted.

5. ACKNOWLEDGMENTS

REFERENCES

Battjes, J.A., 1975. "Modeling of Turbulence in the Surf Zone," in *Proceedings of the Symposium on Modelling Techniques*, ASCE, San Francisco, pp. 1050-1061.

Commander, Naval Surface Force, Pacific and Commander, Naval Surface Force, Atlantic, 1987. *Joint Surf Manual*, COMNAVSURFPAC/COMNAVSURFLANTINST 3840.1B, 02 January 1987.

Earle, M.D., 1989. *Surf Forecasting Software Scientific Reference Manual*, MEC Corporation report for ASW Oceanography Program Office, Naval Ocean Research and Development Activity (N00014-84-C-0116), 261 pp. (Available from Naval Research Laboratory [Code 7032.2], Stennis Space Center, MS 39529-5004.)

Hsu, Y.L., T.R. Mettlach, M.E. Earle, and E. P. Kennelly, 1997. *Interim Report on Validation of the Navy Surf Model*, NRL/MR/7322--97-8054, October 14, 1997.

Hsu, Y.L., T.R. Mettlach, and M.E. Earle, 2000. *Improvement and Validation of the Navy Longshore Current Model*, NRL/FR/7320--00-9927, July 13, 2000.

Lippmann, T.C., A.H. Brookins, and E.B. Thornton, 1996. "Wave Energy Transformation on Natural Profiles," *Coast. Eng.* **27**, 1-20.

Longuet-Higgins, M.S., 1970a. "Longshore Currents Generated by Obliquely Incident Sea Waves," 1, *J. Geophys. Res.* **75**(33), 6678-6789.

Longuet-Higgins, M.S., 1970b. "Longshore Currents Generated by Obliquely Incident Sea Waves," 2, *J. Geophys. Res.* **75**(33), 6790-6801.

Longuet-Higgins, M.S. and J.S. Turner, 1974. "An Entraining Plume Model of a Spilling Breaker," *J. Fluid Mech.* **63**(1), 1-20.

Mettlach, T.R., K.T. Holland, and D.A. May, 1999. *The Accuracy of Navy Surf Model Estimates of Surf Zone Width with an Examination of the Important Influences on Incipient Wave Breaking,* NRL/FR/7440--99-9693, September 24,1999.

Pierson, W.J., Jr. and L. Moskowitz, 1964. "A Proposed Spectral Form for Fully Developed Wind Seas Based on the Similarity Theory of S.A. Kitaigorodskii," *J. Geophys.Res.* **69**(24), 5181-5190.

Reniers, A.J.H.M. and J.A. Battjes, 1997. "A Laboratory Study of Longshore Currents Over Barred and Non-Barred Beaches," *Coast. Eng.* **30**, 1-22.

Ruessink, B.G., J.R. Miles, F. Feddersen, R.T. Guza, and S. Elgar, 2001. "Modeling the Longshore Current on Barred Beaches," *J.Geophys. Res.* **106** (C10), 22451-22463.

Svendsen, I.A., 1984. "Wave Heights and Set-Up in a Surf Zone," *Coast. Eng.* **8**, 303-329.

Svendsen, I.A., 1984. "Mass Flux and Undertow in a Surf Zone," *Coast. Eng.* **8**, 347-364.

Thornton, E.B. and R.T. Guza, 1983. "Transformation of Wave Height Distribution," *J. Geophys.Res.* **88** (C10), 5925-5938.

Thornton, E.B. and R.T. Guza, 1986. "Surf Zone Currents and Random Waves: Field Data and Models," *J. Phys. Oceano.* **16**, 1165-1178.

U.S. Naval Oceanographic Office, 1969. *Breakers and Surf, Principles in Forecasting*, H.O. Pub. No. 234, 56.

Visser, P.J., 1991. "Laboratory Measurements of Uniform Longshore Current," *Coast. Eng.* **15**, 563-591.